ACS NANO
Cite This: ACS Nano 2019, 13, 7359–7365
www.acsnano.org

EDITORIAL

Tutorial on Powder X-ray Diffraction for Characterizing Nanoscale Materials

Powder X-ray diffraction (XRD) is a common characterization technique for nanoscale materials. Analysis of a sample by powder XRD provides important information that is complementary to various microscopic and spectroscopic methods, such as phase identification, sample purity, crystallite size, and, in some cases, morphology. As a bulk technique, the information it provides can be correlated with microscopy data to test if microscopic observations on a small number of particles are representative of the majority of the sample. Despite its importance and ubiquity, the information contained in powder XRD data for nanoscale materials is not always fully harnessed, and in some cases, it is misinterpreted. This Editorial aims to provide the broad nanoscience and nanotechnology communities with a brief tutorial on some of the key aspects of powder XRD data that are often encountered when analyzing samples of nanoscale materials, with an emphasis on inorganic nanoparticles of various sizes, shapes, and dimensionalities. In this way, researchers across many fields, including those who are new to powder XRD or for whom it is not a mainstream technique, can be familiar with key diagnostic features and be better equipped to interpret them in the context of their samples. Readers who wish to learn about powder XRD in more depth and with greater rigor—including the theory, experimental setup, data acquisition protocols, and analysis—are referred to more comprehensive resources.[1−4]

This Editorial aims to provide the broad nanoscience and nanotechnology communities with a brief tutorial on some of the key aspects of powder X-ray diffraction data that are often encountered when analyzing samples of nanoscale materials, with an emphasis on inorganic nanoparticles of various sizes, shapes, and dimensionalities.

We consider CdS as a representative example, as it is a ubiquitous quantum dot material that is widely used in many nanoscience and nanotechnology fields. As nanoparticles, its band gap, and therefore also its color as well as other electronic and optical properties, is dependent upon the size and shape. The most stable crystal structure of CdS is wurtzite, which is shown in the inset to Figure 1. The XRD pattern for bulk CdS, simulated from crystallographic data,[5] is shown in Figure 1. The first three peaks in the CdS XRD pattern correspond to the (100), (002), and (101) planes of CdS, and these are highlighted in the wurtzite crystal structure in the inset to Figure 1. The higher index planes are also labeled on the XRD pattern.

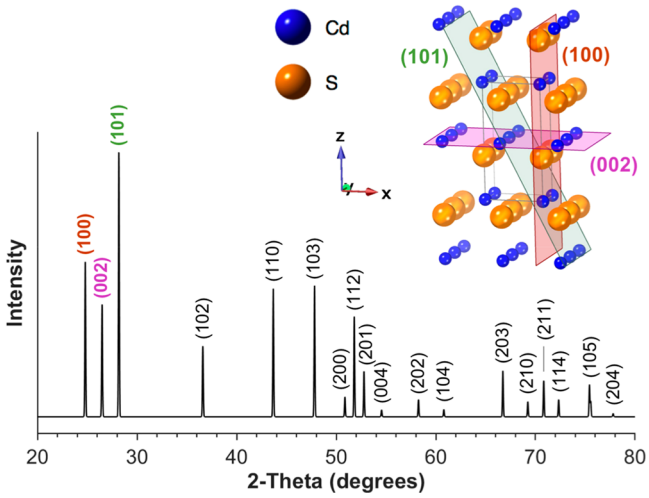

Figure 1. Simulated and indexed powder X-ray diffraction pattern for bulk (1 μm) wurtzite CdS. The inset shows the crystal structure of wurtzite CdS with the (100), (002), and (101) planes highlighted.

When the crystallite size decreases from bulk to nanoscale dimensions, the XRD peaks broaden. The Scherrer equation, $\left(D = \frac{\kappa\lambda}{\beta \cos\theta}\right)$, quantitatively describes the broadening of a peak at a particular diffraction angle (θ), as it relates the crystalline domain size (D) to the width of the peak at half of its height (β).[6] The Scherrer constant, κ, is typically considered to be 0.9[1] but can vary with the morphology of the crystalline domains. The X-ray wavelength (λ) is a constant that depends on the type of X-rays used. Each peak can be evaluated independently and should produce a consistent crystalline domain size as long as the sample can be roughly approximated as uniform, spherical particles. Note that, in the Scherrer equation, the diffraction angle is in radians (not degrees) and corresponds to θ and not 2θ as is typically plotted in an XRD pattern. Also note that crystalline domain size does *not* necessarily correspond to particle size, as particles can be polycrystalline, containing multiple crystalline domains. When the crystalline domain size calculated by the Scherrer equation matches the average diameter of particles determined by transmission electron microscopy (TEM) or other particle sizing methods, this observation suggests that the particles are single crystals rather than polycrystalline.

Figure 2 shows the same bulk XRD pattern for wurtzite CdS that was shown in Figure 1, along with XRD patterns for CdS having smaller crystalline domain sizes. As the size decreases

Published: July 23, 2019

DOI: 10.1021/acsnano.9b05157
ACS Nano 2019, 13, 7359–7365

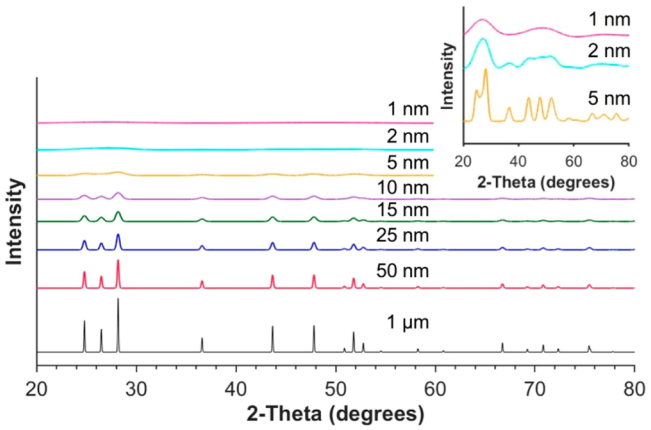

Figure 2. Simulated powder X-ray diffraction patterns for wurtzite CdS spherical particles of different sizes that range from 1 μm to 1 nm. The inset shows the 1, 2, and 5 nm XRD patterns on an expanded *y*-axis scale for clarity.

from bulk (approximated as 1 μm) to 50 nm, slight peak broadening is observed. It is difficult to calculate crystalline domain sizes using the Scherrer equation for particles in this size range, as most of the peak broadening is due to instrumental effects rather than particle size effects; careful analysis (*i.e.*, full profile fitting) is required to deconvolute these two independent contributors. Decreasing crystalline domain size from 50 to 25 nm causes more noticeable peak broadening. As crystalline domain size decreases further, peak broadening increases significantly. Below 10 nm, peak broadening is so significant that signal intensity is low and peaks overlap and can be difficult to discern. Particles having crystalline domain sizes below 5 nm become difficult to analyze, due to both broad peaks and low signal-to-noise ratios. Size-dependent XRD peak broadening has important implications for nanomaterial characterization. For example, if TEM analysis shows spherical particles having an average diameter of 10 nm, but the XRD pattern has sharp peaks that are more consistent with particles having much larger crystalline domain sizes, then the majority of the bulk sample is *not* composed of 10 nm particles; it is more likely that the microscopically observed 10 nm particles represent only a minority subpopulation.

Not all nanoscale particles can be approximated by spheres, and powder XRD data can look different for particles of the same material that have different morphologies. The peak positions (*i.e.*, *x*-axis values) will remain the same, but the relative intensities of the peaks (*i.e.*, *y*-axis values) can change. For spherical particles, drying them to form a powder randomly orients them, and there is a statistically random distribution of crystal plane orientations with respect to the diffraction angle (Figure 3a). As a result, the relative intensities of all peaks are those expected based on the simulated diffraction pattern of the bulk powder, as shown in Figures 1 and 2. Note that peak broadening relates to the widths of the peaks, whereas the relative intensities relate to the height, so XRD patterns for spherical particles of nanoscale dimensions will have the same relative intensities as the bulk material, but the peaks will be broadened.

As particle shapes become nonspherical, there is a chance that, upon drying, they will orient in nonrandom directions. For example, a sample of cube-shaped particles dried or precipitated from solution will tend to orient with their flat faces parallel to the drying surface (Figure 3b). It is much less likely that nanocubes would dry with their corners or edges touching the drying surface, and therefore, the powder of nanocubes will be preferentially oriented in the crystallographic direction corresponding to the faces. Similarly, one-dimensional (1D) nanowires will tend to orient flat on a substrate upon drying (Figure 3c). Other particle shapes, such as octahedra or tetrahedra, may have different ways of orienting. The majority of the sample may exhibit preferred orientation, or only a fraction of it may, depending on the quality and size of the various particle shapes. In addition, the method in which the sample was dried to form a powder and/

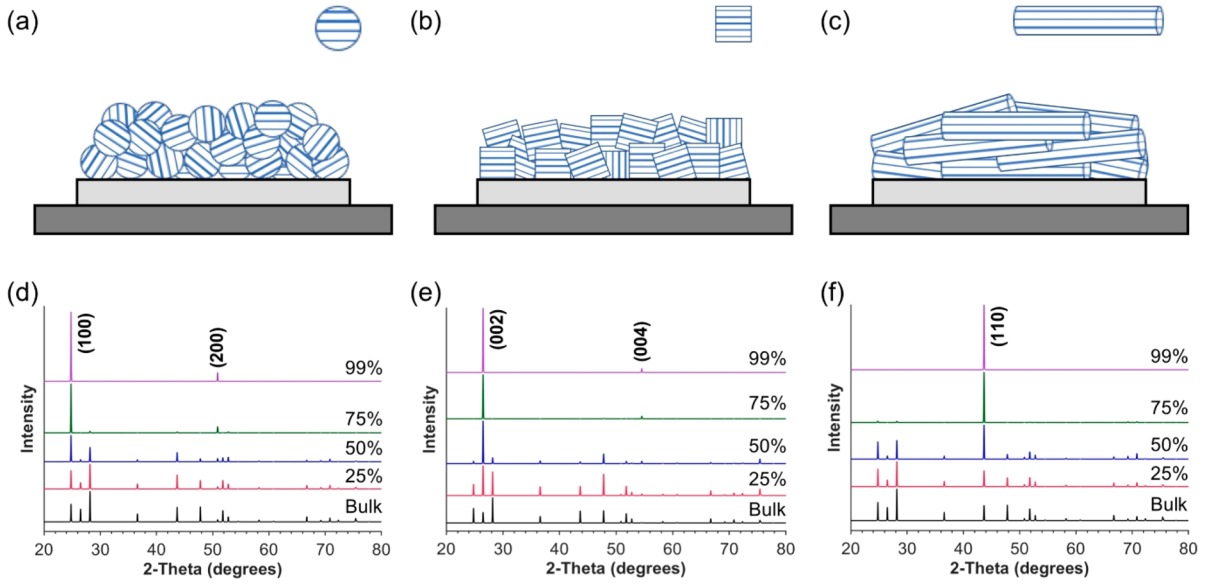

Figure 3. Graphical representation of preferred orientation for nanoparticles having different shapes: (a) spheres, (b) cubes, and (c) rods. Simulated X-ray diffraction patterns for varying degrees of alignment (*i.e.*, preferred orientation) of wurtzite CdS particles along specific crystallographic directions: (d) [100], (e) [001], and (f) [110].

DOI: 10.1021/acsnano.9b05157
ACS Nano 2019, 13, 7359−7365

or how the XRD sample was prepared can influence the preferred orientation of the sample.

Figure 3d–f shows XRD patterns for wurtzite CdS corresponding to three distinct preferred orientation directions at various levels of alignment. First consider particles of CdS that are oriented along the [100] direction (Figure 3d). At the extreme limit, where all particles are aligned with their (100) faces parallel to the surface of the XRD sample holder, the only observable peaks will be those corresponding to the {*h*00} crystal planes that are parallel to (100), including (200), (400), *etc.* At intermediate levels of alignment, the intensities of the {*h*00} family of crystal planes will be enhanced relative to those of other planes [{*hkl*}, {*hk*0}, {00*l*}, *etc.*] because a larger-than-random fraction of particles is oriented in this direction.

Similar preferred orientation effects emerge for alignment in other crystallographic directions but with different relative peak intensities. For example, Figure 3e shows XRD patterns for wurtzite CdS that exhibit preferred orientation along the [001] direction. Here, it is the {00*l*} peaks that are enhanced as the extent of alignment increases. Figure 3f shows XRD patterns corresponding to preferred orientation of wurtzite CdS along the [110] direction. Figure 3 highlights some of the ways in which preferred orientation can produce XRD patterns with different relative peak intensities than expected based on simulated or database patterns that correspond to crystallites oriented in a statistically random way, that is, bulk powders composed of nominally spherical particles. Likewise, XRD patterns for the same material, such as wurtzite CdS, can have a range of possible relative intensities depending on the direction and degree of alignment of particles in the XRD sample. The key to recognizing preferred orientation effects on relative peak intensities is to index the XRD pattern fully, that is, assign the (*hkl*) values to each peak and look for enhancements in the relative intensities of related families of planes, such as (110), (220), (330), *etc.*

To test if different relative intensities are due to preferred orientation effects, the same sample can sometimes be prepared for XRD analysis in ways that either minimize or maximize preferred orientation. For example, Figure 4 shows the crystal structure of GeS, along with a TEM image of GeS nanosheets.[7] The corresponding XRD patterns in Figure 4 show experimental data for the GeS nanosheets drop-cast onto the XRD sample holder, which results in significant preferred orientation because the nanosheets tend to lie parallel to the surface of the sample holder. Figure 4 also shows experimental XRD data for the exact same GeS nanosheet sample that was first dried as a powder and mixed carefully to minimize preferred orientation. Simulated XRD patterns for bulk GeS (with no preferred orientation) and fully oriented GeS are also shown in Figure 4. The experimental XRD patterns are distinct, and comparison with the simulated XRD patterns indicates that the drop-cast sample shows almost full preferred orientation whereas the powder sample shows only partial preferred orientation. X-ray diffraction patterns of the same sample prepared in different ways should have different relative intensities, corresponding to enhancement of related families of planes. Such comparisons can help to validate claims that a bulk sample contains predominantly nanosheets (or other two-dimensional [2D] morphologies). Similar approaches can be applied to other morphologies, including 1D nanowires.

Nanomaterial samples that include multiple distinct subpopulations of different sizes and/or shapes can produce more complex XRD patterns. For example, Figure 5 shows the

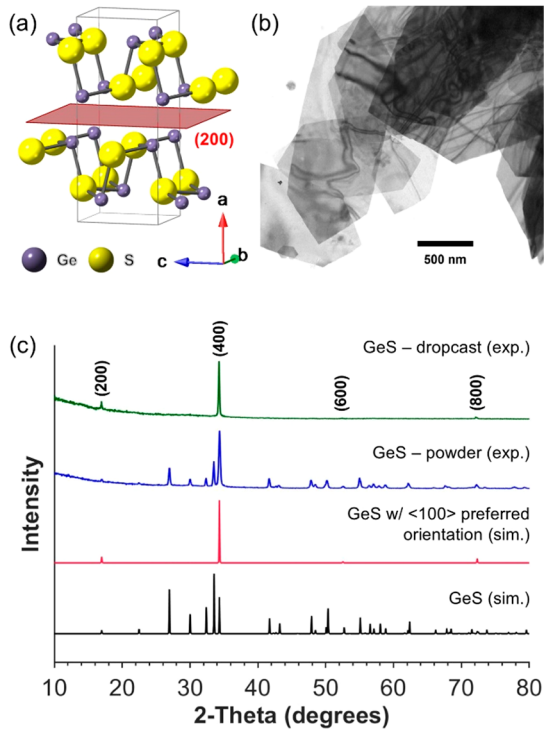

Figure 4. (a) Crystal structure of GeS and (b) transmission electron microscope image of GeS nanosheets. (c) Powder X-ray diffraction patterns showing significant preferred orientation in the [100] direction when GeS nanosheets are drop-cast (green) and only minimal preferred orientation when prepared as a powder (blue). Two simulated reference patterns, with (red) and without (black) preferred orientation, are shown for comparison. Adapted from ref 7. Copyright 2010 American Chemical Society.

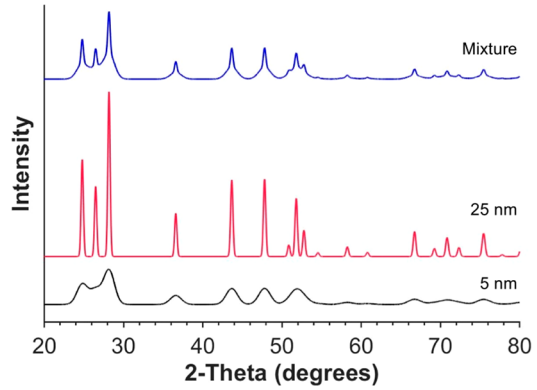

Figure 5. Simulated wurtzite CdS powder X-ray diffraction patterns of (bottom) 5 nm particles, (middle) 25 nm particles, and (top) a mixture that contains 75% 5 nm particles and 25% 25 nm particles.

simulated powder XRD pattern for a sample containing 75% 5 nm wurtzite CdS particles and 25% 25 nm wurtzite CdS particles. This bimodal particle size distribution produces peak shapes that contain narrower tips, from the contribution of the 25 nm particles having less peak broadening, and broader tails, from the contribution of the 5 nm particles having more peak broadening. As another example, consider nanoplates of wurtzite CoS that have average dimensions of 13 nm × 5 nm and have the (001) plane as the base of the nanoplate (Figure 6).[8] Here, the crystalline domain size corresponding to

DOI: 10.1021/acsnano.9b05157
ACS Nano 2019, 13, 7359–7365

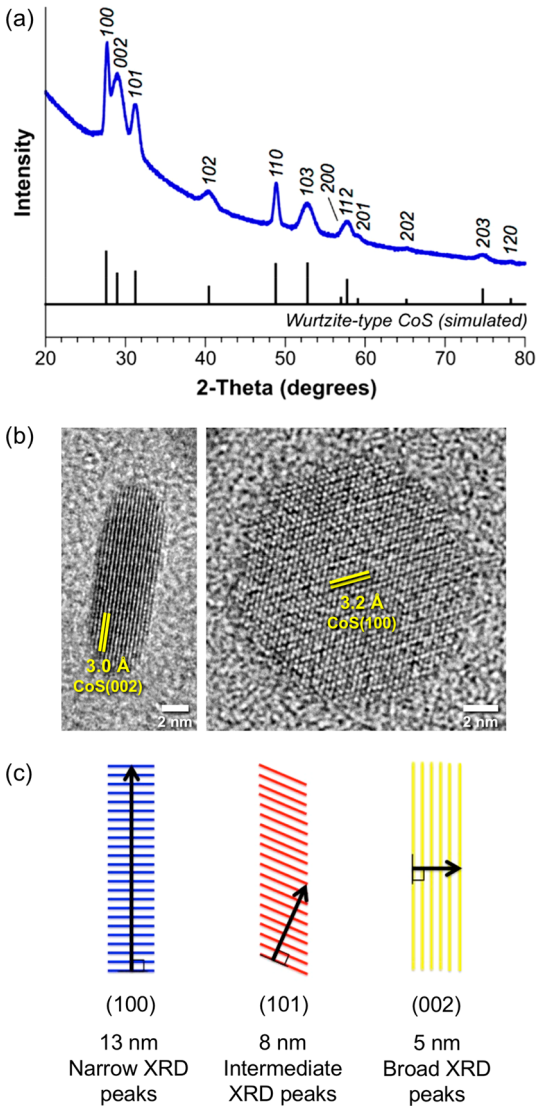

Figure 6. (a) Experimental and simulated powder XRD patterns for platelet-shaped wurtzite CoS nanoparticles. (b) High-resolution transmission electron microscope images of a CoS nanoplatelet viewed from the (left) side and (right) top. (c) Representation of the different effective thicknesses (*i.e.*, crystalline domain sizes) in different directions of the nanoplates, which correlate with different peak widths in the experimental XRD pattern. Adapted from ref 8. Copyright 2016 American Chemical Society.

the {00*l*} peaks is 5 nm, so the (002) and related {00*l*} peaks will have peak broadening that is consistent with a 5 nm crystallite. However, the crystalline domain size corresponding to the {*h*00} peaks is 13 nm, so the (100) and related {*h*00} peaks will have peak broadening that is consistent with a 13 nm crystallite. As a result, the (100) and (002) peaks, which are close to each other, have significantly different widths. The (101) peak has intermediate width, as it corresponds to a crystal plane that is oriented diagonally along the particle (Figure 6). The differences in peak broadening for different families of planes are consistent with the dimensions and crystal orientation that are observed microscopically, which reconciles the microscopic and bulk data to confirm that the nanoplate morphology comprises the majority of the sample. Note that, in the wurtzite CoS case, preferred orientation in the XRD pattern was purposely minimized by preparing the sample by a method that did not allow the nanoplates to align extensively.

Finally, consider a mixture of different crystalline forms of CdS. Although CdS prefers to crystallize in the hexagonal wurtzite structure, the cubic zinc blende polymorph is also known[9] and can be present in samples. Figure 7 shows

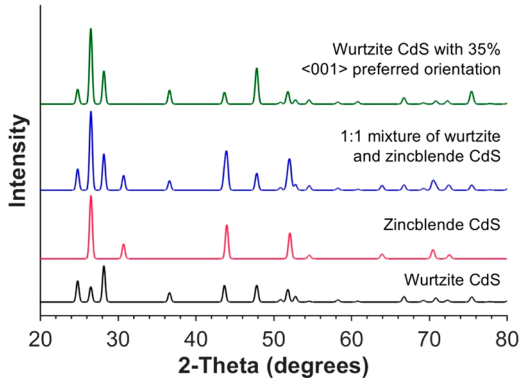

Figure 7. Simulated powder X-ray diffraction patterns for 20 nm particles of wurtzite and zinc blende CdS. A simulated pattern for a 1:1 mixture of wurtzite and zinc blende CdS is also shown, along with wurtzite CdS that has 35% preferred oriented in the [001] direction.

simulated XRD patterns for wurtzite CdS and zinc blende CdS, along with a 1:1 mixture of the wurtzite and zinc blende phases, both as 20 nm spherical particles. The zinc blende peaks overlap with some of the wurtzite peaks, so the XRD pattern of the mixture appears to have higher relative intensities, relative to wurtzite, for the peaks to which the zinc blende phase contributes. Figure 7 also shows the XRD pattern for a sample containing 20 nm nanoplates of wurtzite CdS that have 35% preferred orientation in the [001] direction. It is important to note that these two XRD patterns—a mixture of zinc blende and wurtzite CdS and pure wurtzite CdS with partial preferred orientation along the [001] direction—appear very similar. The first three peaks are almost identical in relative intensity, and subtle features differentiate the two, including the presence or absence of a few low-intensity peaks (*i.e.*, a peak near 31°) and the relative intensities of some of the higher-angle peaks. Careful analysis is therefore required to differentiate scenarios that can lead to similar XRD patterns.

Nanosheets, which are ubiquitous in 2D materials research, present an extreme case of both crystalline domain size and preferred orientation effects. Consider an atomically thin nanosheet that has lateral dimensions on the order of 100 nm. The crystalline domain size in all directions of the nanosheet, except for the crystal plane that it contains, will be on the order of, and sometimes smaller than, 1 nm. As can be seen in the XRD patterns in Figure 2, peaks for such small crystalline domain sizes are so broad that they are not observable. If such thin nanosheets are precipitated, they will almost assuredly exhibit significant preferred orientation such that they will stack vertically but in a random way. To visualize this, consider a deck of cards. If a deck of cards is thrown up in the air and the cards are allowed to settle on the floor, they will be stacked vertically on top of each other, but they will be misaligned and in random orientations laterally. A similar scenario occurs when exfoliated nanosheets are restacked, either through

DOI: 10.1021/acsnano.9b05157
ACS Nano 2019, 13, 7359−7365

precipitation or deposition on a surface. Applied to XRD of nanosheets, the effective crystalline domain size is small and the system contains significant disorder. Thin nanosheets are often buckled when restacked as a powder, and their stacking periodicity has disorder due to this buckling. Diffraction peaks arising from stacked nanosheets therefore will not be sharp, and the most intense diffraction peaks (for samples exhibiting significant preferred orientation) will correspond to the average distance between nanosheets. For atomically thin nanosheets that are allowed to precipitate in analogy to how cards restack, the XRD pattern will simply be a series of broad {00*l*} peaks. For thicker and more rigid nanosheets, like the GeS system shown in Figure 4, the stacking can become more uniform and the nanosheets can be sufficiently thick to show XRD patterns that can look more like nanoplates with preferred orientation. However, it is worth noting that restacking of exfoliated nanosheets is *unlikely* to yield a precipitate that exactly matches that expected for the bulk material from which it was derived. The nanosheets are unlikely to stack with perfect vertical and lateral alignment—such an achievement would be quite notable! Therefore, the XRD pattern for exfoliated and restacked nanosheets, if they comprise the majority of the sample, should not match that of the bulk material.

Given the considerations outlined above, it is notable that XRD patterns for samples of nanoparticles having different sizes and shapes can look different, and careful analysis of the XRD data can provide useful information and also help correlate microscopic observations with the bulk sample. Electron diffraction patterns, which can be acquired during TEM analysis, can be compared with XRD patterns of the bulk sample to confirm that the particles being imaged are those that comprise the majority of the sample.

X-ray diffraction (XRD) patterns for samples of nanoparticles having different sizes and shapes can look different, and careful analysis of the XRD data can provide useful information and also help correlate microscopic observations with the bulk sample.

There are also other considerations to keep in mind when analyzing powder XRD data that are especially relevant for nanoscale materials.

Phase Identification. One application of powder XRD is phase identification, which is often accomplished by comparing an experimental XRD pattern with a reference pattern that is either simulated or obtained from a database. In such cases, an unambiguous and complete match between the experimental and reference patterns is needed. Arbitrary peaks predicted by a reference pattern cannot be missing in the experimental XRD data without justification. All peaks in the reference pattern, which includes both of their diffraction angles and intensities, should be accounted for in the experimental pattern unless there is a clear and justified rationale for why certain peaks may be missing or have different intensities, such as preferred orientation, as discussed above. To accomplish this comparison, experimental XRD patterns having sufficient signal-to-noise ratios are needed so that low-intensity peaks can be observed.

Phase identification by XRD for some systems, especially nanoscale materials, can be particularly challenging because of nearly indistinguishable diffraction patterns. For example, Au and Ag are both face-centered cubic metals that have sufficiently similar lattice constants that Au and Ag nanoparticles (which have broadened peaks) cannot be differentiated by XRD. Similarly, the XRD patterns of two forms of iron oxide, magnetite (Fe_3O_4) and maghemite (γ-Fe_2O_3), are sufficiently similar that, for nanoparticles with broad peaks, they cannot be distinguished by XRD. Differentiating the hexagonal close-packed form of elemental nickel from hexagonal nickel carbides (Ni_3C) and nitrides (Ni_3N) can be similarly challenging. In these and other cases, additional characterization techniques are important for achieving phase identification.

X-ray Diffraction Databases *vs* Simulated Reference Patterns. Reference XRD patterns can be obtained from several sources. Commercially available powder diffraction databases are excellent resources of broad scope that are often available with the software used to analyze experimental XRD data. When reference patterns from such databases are used to compare with experimental data, the specific reference file identification number should be given, as there are often multiple entries for the same phase. It is also worth noting that relative peak intensities of database patterns can sometimes differ from those observed experimentally. For example, database patterns based on older crystallographic data could include semiquantitative peak intensities (*i.e.*, very strong, strong, medium, weak, very weak, *etc.*), which were determined by rough quantitation of diffraction lines on films that were used prior to the availability of digital detectors.

Powder XRD patterns can also be simulated directly from crystallographic data, and software programs that can do this often are also capable of including preferred orientation and peak broadening due to nanoscale crystalline domains. In these cases, it is important to cite the reference from which the crystallographic data were obtained. It is also important to make sure that all crystallographic data have been entered into the simulation program correctly. Errors in data entry—including obvious errors such as typos in fractional coordinates and less obvious errors such as omission of fractional site occupancies and use of nonstandard space group settings—can lead to errors in the simulated patterns. Crystallographic information files (CIFs) can also be downloaded and used to simulate XRD patterns, thereby avoiding manual data entry. Here, it is important to understand the source of the CIF and its reliability and/or feasibility. For example, journals that include CIFs as part of the Supporting Information for manuscripts often require CIF checks prior to acceptance, thereby helping to ensure that they are reasonable. Crystallographic information files generated from computationally derived databases are also useful, but it is important to know if the CIF files correspond to known, stable phases that have been experimentally validated or if they correspond to previously unknown and/or metastable phases that are unlikely to be the products of routine syntheses and, therefore, would require additional characterization and justification to confirm that they formed.

Amorphous *vs* Nanocrystalline Products. X-ray diffraction is a powerful characterization tool for identifying crystalline phases in a sample, but one important limitation involves amorphous components that lack long-range crystallographic order, as they do not produce diffraction patterns with

DOI: 10.1021/acsnano.9b05157
ACS Nano 2019, 13, 7359−7365

discernible peaks. An XRD pattern for a sample that contains a significant impurity of an amorphous component, in addition to one or more nanoscopic crystalline components, may look indistinguishable from a similar sample containing only the nanocrystalline component(s). Additional characterization is therefore needed to test sample purity and/or to determine whether or not some of the sample is amorphous. It is worth noting that XRD patterns for amorphous phases can appear similar to those observed for nanoparticles having diameters that are less than 2 nm; both would exhibit similar, significant peak broadening.

Sample Purity. As noted above, sample purity determination can require several characterization tools. Along these lines, it is also important to consider the limits of detection and quantification of typical laboratory X-ray diffractometers, which can be on the order of 5−10%. These are just approximate values, and they can vary significantly depending on the instrument and the sample being characterized. Samples that produce XRD patterns having low signal-to-noise ratios, including poorly crystalline materials and nanoscale materials having significantly broadened peaks, can contain large amounts of components that do not produce XRD peaks that rise significantly above the background noise. Low-intensity peaks, which may correspond to impurities, can also be difficult to observe. The presence of asymmetric peaks may be due to stacking faults and other defects or a distribution of compositions in compounds that could be present as alloys or solid solutions.

Lattice Constants. For highly crystalline bulk materials with high signal-to-noise ratios and sharp peaks, lattice constants (in units of Å) are often reported to three or four decimal places, with the uncertainty (error) corresponding to the last decimal place. To obtain such precise values, profile fitting and refinement are required. For nanocrystalline materials, which have lower signal-to-noise ratios and broad peaks, such precision in lattice constants is difficult to achieve. Reported lattice constants are therefore not expected to contain three or four decimal places unless rigorous and reliable profile fitting and refinement were carried out (and even then, such precision may not be possible). To identify trends in lattice constants across multiple related samples, such as alloys of systematically varying compositions, it is sometimes necessary to include an internal standard in the samples for calibration purposes. For example, by including small amounts of a bulk crystalline compound such as LaB_6 in samples of alloy nanoparticles (assuming that the LaB_6 peaks do not overlap significantly with those from the nanoparticles), the XRD patterns of the alloy nanoparticles can be compared more accurately by applying a zero-point shift so that the LaB_6 peaks all overlap. (A zero-point shift involves minor shifting of the *x*-axis, for legitimate reasons caused by errors such as sample height alignment, that is achieved by adding or subtracting a very small constant value.) In this way, any changes in the peak positions arising from the sample can be considered reliable because they change relative to those of the internal standard, which remain fixed.

Vegard's Law. Changes in composition can change the properties of many types of nanoscale materials. For example, Au−Ag alloy nanoparticles have a surface plasmon resonance energy that depends on the relative amounts of Au and Ag alloyed in the nanoparticle. Likewise, the emission energy (color) of semiconductor quantum dots can tuned by composition, that is, by substituting some of the Cd or S in CdS nanoparticles with Zn or Se, respectively. Powder XRD data for such solid−solution nanoparticles typically reveal lattice constants that are intermediate between the end members. Vegard's law is the empirical observation that there is often a linear relationship between the lattice constants (and in some cases properties) of an alloy and its composition.[1] For example, Vegard's law would predict that the lattice constant for a $Au_{0.5}Cu_{0.5}$ alloy would be the average of the lattice constants of Au and Cu. Because of this relationship, XRD is often used to determine composition, and composition is used to predict lattice constants. It is important to remember that Vegard's law is not a law but rather an empirical relationship that often has deviations. It is useful as a rough estimate, but it has limitations. Therefore, it is best used in conjunction with other characterization techniques that can accurately measure composition.

It is important to recognize the capabilities and limitations of powder XRD for nanoscale materials when collecting and analyzing data as well as to ensure that claims based on XRD data are accurate, appropriate, and not overreaching.

Powder XRD provides useful information about structure, phase, composition, shape, size, crystallinity, and other important features of nanoscale materials, although unambiguous sample characterization almost always requires complementary experimental and/or computational methods. Powder XRD data for nanoscale materials can often be straightforward to analyze for the key information that is needed, but other times, it can be quite complex. This tutorial highlighted several key features of XRD patterns that are often encountered in nanoscale materials as well as diagnostic insights that we hope will be helpful in interpreting data. However, the selected topics were by no means exhaustive nor did the discussions capture all aspects of data collection and analysis, including subtle (but important) nuances that require full-profile fitting and refinement to identify, to quantify, and to deconvolute. In the end, it is important to recognize the capabilities and limitations of powder XRD for nanoscale materials when collecting and analyzing data as well as to ensure that claims based on XRD data are accurate, appropriate, and not overreaching.

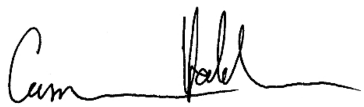

Cameron F. Holder
The Pennsylvania State University

Raymond E. Schaak,* Associate Editor
The Pennsylvania State University

AUTHOR INFORMATION

Corresponding Author
*E-mail: res20@psu.edu.

DOI: 10.1021/acsnano.9b05157
ACS Nano 2019, 13, 7359−7365

ORCID

Cameron F. Holder: 0000-0003-1036-4142

Raymond E. Schaak: 0000-0002-7468-8181

Notes

Views expressed in this editorial are those of the authors and not necessarily the views of the ACS.

REFERENCES

(1) Cullity, B. D. *Elements of X-ray Diffraction*, 3rd ed.; Prentice Hall: Upper Saddle River, NJ, 2001.

(2) Hammond, C. *The Basics of Crystallography and Diffraction*, 4th ed.; Oxford University Press: Oxford, UK, 2015.

(3) Snyder, R. L.; Jenkins, R. *Introduction to X-ray Powder Diffractometry*; Wiley: New York, 1996.

(4) Warren, B. E. *X-ray Diffraction*; Addison-Wesley: Reading, MA, 1969.

(5) Villars, P. *Pearson's Handbook Desk Edition*; ASM International: Materials Park, OH, 1997.

(6) Scherrer, P. Bestimmung der Grösse und der Inneren Struktur von Kolloidteilchen Mittels Röntgenstrahlen. *Göttinger Nachrichten Gesell.* **1918**, *2*, 98−100.

(7) Vaughn, D. D.; Patel, R. J.; Hickner, M. A.; Schaak, R. E. Single-Crystal Colloidal Nanosheets of GeS and GeSe. *J. Am. Chem. Soc.* **2010**, *132*, 15170−15172.

(8) Powell, A. E.; Hodges, J. M.; Schaak, R. E. Preserving Both Anion and Cation Sublattice Features during a Nanocrystal Cation-Exchange Reaction: Synthesis of Metastable Wurtzite-Type CoS and MnS. *J. Am. Chem. Soc.* **2016**, *138*, 471−474.

(9) Cao, Y. C.; Wang, J. One-Pot Synthesis of High-Quality Zinc-Blende CdS Nanocrystals. *J. Am. Chem. Soc.* **2004**, *126*, 14336−14337.

DOI: 10.1021/acsnano.9b05157
ACS Nano 2019, 13, 7359−7365